First Principles Study of Adsorption and Dissociation of CO on W(111)

Liang Chen,[†,‡] David S. Sholl,[†,§] and J. Karl Johnson*[,†,‡]

National Energy Technology Laboratory, Pittsburgh, Pennsylvania 15236, Department of Chemical Engineering, University of Pittsburgh, Pittsburgh, Pennsylvania 15261, and Department of Chemical Engineering, Carnegie Mellon University, Pittsburgh, Pennsylvania 15213

Received: September 21, 2005; In Final Form: November 17, 2005

The adsorption and dissociation of carbon monoxide on the W(111) surface is studied with density functional theory. The CO molecule is found to adsorb in end-on configurations (α states) and inclined configurations (β states). The dissociation of the most strongly bound β state CO is found to have an activation energy of about 0.8 eV, which is lower than the energy required to desorb CO molecularly from the surface. The diffusion of CO and O on W(111) is predicted to be facile at room temperature, whereas C atoms are virtually immobile up to ~600 K, according to our calculations. Preadsorbed carbon atoms are shown to prevent the dissociation of CO by blocking the most strongly bound β state adsorption site and by blocking the dissociation pathway. We predict that dissociation of CO on W(111) is a self-poisoning process.

I. Introduction

CO adsorption on tungsten and modified tungsten surfaces has been studied both experimentally and theoretically because of their potential use in methanol reforming and fuel cell technology.[1,2] Temperature programmed desorption (TPD) of CO on most transition metal surfaces shows a low temperature α state and several high temperature β states. In the conventional picture of CO binding to transition-metal surfaces,[3−5] The α state is assigned to CO adsorbed in an end-on orientation with the carbon end toward the surface, while the β state is assigned to the species adsorbed in an orientation that is tilted with respect to the surface normal and with both C and O interacting with the surface. Chen and co-workers[6] studied CO and H_2O adsorbed on W(111), C/W(111), and C/O/W(111) surfaces using TPD and high-resolution electron energy loss (HREEL) spectroscopy. They observed desorption and vibrational spectra. Their results imply that the α state CO desorbs molecularly from clean W(111) at about 293 K, while the low frequency β state CO dissociates at room temperature, and recombines to form molecular CO around 870 K. In contrast, dissociation is not observed for CO on the carbon modified W(111) surface, denoted as C/W(111). Lee and co-workers[7] have reported TPD, ultraviolet photoelectron spectroscopy, and X-ray photoelectron spectroscopy experiments for CO adsorption on the clean W(111) surface. In contrast to the work of Chen et al., they suggested that β state CO molecules do not dissociate.[7]

We have found only one theoretical study of CO on the W(111) surface in the literature.[8] Ryu et al. used the atom superposition and electron delocalization molecular orbital theory,[9,10] which is a corrected extended Hückel method, in their calculations. They used only three layers of atoms in their model, which is the minimum possible number of layers for a bcc (111) surface. Ryu et al. studied the energetics of CO adsorbed on various binding sites and configurations. Their reported binding energies are much higher than experimental values inferred from TPD.[6] Furthermore, they claimed that it is unclear if the β state CO leads to dissociation. In the present paper, we have used first principles density functional theory (DFT) to study the adsorption of CO on the W(111) surface. We have computed binding energies, vibrational frequencies, and diffusion and dissociation pathways of CO on clean and carbon preadsorbed W(111) surfaces. We compare our results with experimental data where possible.

II. Theoretical Calculations

Density functional theory calculations were performed with use of the generalized gradient approximation. The Vienna ab initio simulation package[11−13] was used for all calculations. The revised Perdew Burke Ernzerhof (rPBE)[14,15] exchange-correlation functional was used because we found that the PW91 functional[16] gave binding energies for CO on W(111) that were 0.2−0.4 eV greater than those computed from the rPBE functional. It is known that PW91 predicts binding energies for CO on metal surfaces that are too high compared with experiments.[17] The electron−ion interactions were described by PAW (Projector Augmented Wave) pseudopotentials.[18,19] Electron smearing was employed with use of the Methfessel−Paxton technique, with a smearing width of $\zeta = 0.1$ eV, to minimize the errors in the Hellmann−Feynman forces due to the electronic free energy. All calculated energies are extrapolated to $T = 0$ K.

The Brillouin zone was sampled with 13 irreducible k-points ($5 \times 5 \times 1$ mesh) generated from the Monkhorst−Pack scheme.[20] We have tested the k-point convergence by comparing calculations with 54 and 13 irreducible K-points. We found the energy to be converged to within 0.01 eV. An energy cutoff of 400 eV was used in all calculations. The rPBE calculated lattice constant for bulk tungsten is 3.18 Å, which agrees well with the experimental values of 3.17 Å. The calculated gas-phase CO bond length is 1.14 Å, which also agrees well with the experimental value of 1.13 Å.

* Address correspondence to this author. E-mail: karlj@pitt.edu.
† National Energy Technology Laboratory.
‡ University of Pittsburgh.
§ Carnegie Mellon University.

10.1021/jp055374z CCC: $33.50
Published on Web 12/23/2005

TABLE 1: Interlayer Relaxation of the W(111) Surface as a Function of the Number of Layers in the Model[a]

no. of layers	thickness (Å)	F_{12} (%)	F_{23} (%)	F_{34} (%)	F_{45} (%)
6	14.57	−13.5	−10.5	−18.5	
7	15.48	−19.9 (−17.5)	−23.8 (−14.5)	18.1 (11.2)	
9	17.31	−23.3 (−23.5)	−21.4 (−17.4)	14.2 (22.0)	−1.4 (−5.5)
11	19.14	−24.6	−23.8	18.1	−3.5

[a] The data in parentheses are cited from the literature.[24] F_{ij} denotes the fractional change in the layer spacing of the relaxed thin films.

TABLE 2: Interlayer Relaxation of the (001) and (110) Surfaces of W[a]

surfaces	F_{12} (%)	exptl[23]	F_{23} (%)	exptl[23]
(001)	−8.04	−7	4.54	3.9
(110)	−3.08	−2.1	0.87	0.7

[a] F_{ij} denotes the fractional change in the layer spacing of the relaxed thin films. Experimentally measured data from Xu and Adams[23] are also shown.

The binding energy is defined as $E_b = E_a + E_{slab} - E_{a/slab}$, where the three terms on the right-hand side are the energy of an isolated molecule or atom, the energy of the clean W(111) surface, and the energy of the slab with the adsorbed molecule or atom, respectively. A positive value for E_b corresponds to stable adsorption with this definition.

Vibrational frequencies were calculated by diagonalizing the Hessian matrix of selected atoms. The Hessian matrix was calculated within VASP by a finite difference method. The atoms in the top four W layers and CO were independently displaced by 0.02 Å along each Cartesian coordinate direction. We compared C−O stretching frequencies calculated by allowing all W atoms in the first four layers to move with those computed by fixing all W atom positions. The C−O frequencies were the same to within a few wavenumbers, indicating that coupling of the C−O vibration to the underlying W lattice is negligible.

The nudged elastic band (NEB) method of Jónsson and coworkers[21,22] was used to compute diffusion and dissociation pathways. Initial and final states were chosen and the number of images was increased to achieve a smooth curve. At least eight images were used for each calculation.

III. Results and Discussions

A. Surface Relaxation. We begin by discussing the surface relaxation of the clean W(111) surface as a function of the number of layers. In each calculation, we used a supercell containing a 10 Å vacuum space and kept the bottom three layers fixed. The surface relaxation was characterized by monitoring the interlayer relaxation with respect to the bulk interlayer spacing. The interlayer spacing is 0.914 Å for the unrelaxed W(111) surface. Note that this is much smaller than that of the W(100) slab, which is 1.59 Å. Table 1 presents the calculated relaxation of the W(111) slab and the thickness of the supercell. F_{ij} is the fractional change in the layer spacing. A triplet relaxation pattern was found with substantial contraction of the first two layer spacings and expansion of the third layer spacing. In contrast, the relaxation of other low-index surfaces is relatively small and follows a different oscillatory pattern. We have calibrated the accuracy of our DFT calculations by computing the relaxation of the W(110) and W(001) slabs and comparing our calculations with experimental data. Table 2 summarizes the calculated and experimentally measured[23] relaxation of the (110) and (001) surfaces. The agreement between experiments and calculations is excellent, giving us confidence in our W(111) results. The unusual relaxation pattern of (111) surfaces has been studied by Xu and co-workers using tight-binding and local density approximation DFT.[23,24] There are no experimental data for interlayer relaxation of the W(111) surface, to the best of our knowledge.

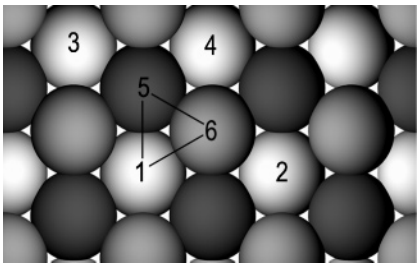

Figure 1. Schematic of the W(111) surface. The triangle represents the reduced unit cell. Light spheres (labeled 1−4) are the first layer W atoms, the black spheres (e.g., 5) represent second layer W atoms, and the gray spheres (e.g., 6) represent the third layer W atoms.

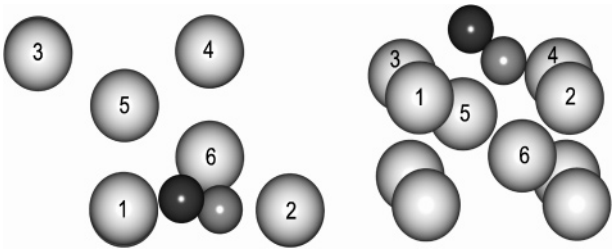

Figure 2. The inclined CO (β) state with the highest binding energy. The left figure is the top view and the right figure is the side view. The black sphere is oxygen and the gray sphere is carbon. Only the top four W layers are shown.

The data in Table 1 indicate that a large supercell with at least seven layers is necessary to accurately model the surface relaxation of W(111). A model containing only six layers predicts that all relaxed layers will contract (see Table 1). This is mainly due to the very small interlayer spacing along the ⟨111⟩ direction of bcc metals. The data in Table 1 also indicate that the calculated results with seven layers are well converged; including more layers does not improve the accuracy dramatically. In the subsequent calculations, therefore, we chose to use a supercell containing seven W layers and a vacuum spacing of 10 Å.

B. CO Adsorption. We have calculated the binding energies and vibrational frequencies of CO adsorbed on the W(111) surface in various binding sites and configurations. Figure 1 shows a schematic of the W(111) surface; the triangle represents the reduced unit cell. The light spheres, numbered 1−4, represent the first layer W atoms, while the medium and dark colored spheres, numbered 5 and 6, represent the second and third layer W atoms, respectively. We have investigated three end-on (α) configurations and four inclined (β) configurations for CO bound to the W(111) surface. The top and side views of the most favorable inclined adsorption configuration, C-2:O-1, are shown in Figure 2. The notation for inclined adsorption, C-*n*:O-*m*, indicates that the carbon is interacting with the *n*th W atom, while oxygen is interacting with the *m*th W atom as numbered in Figures 1 and 2. Only fours layers are shown in Figure 2, although seven layers were used in the calculations.

TABLE 3: Binding Energy (eV) of CO Adsorbed on the W(111) Surface as a Function of the Number of Layers[a]

	no. of layers						
Site	3	4	5	6	7	8	3[a]
1-fold	2.46	2.23	1.37	1.40	1.37	−	2.89
3-fold shallow	2.15	2.21	1.43	1.37	1.37	−	2.53
3-fold deep	1.49	1.35	1.41	1.05	0.89	0.93	1.99
inclined C-2:O-1				2.14	1.79	1.74	4.5

[a] Data from Ryu et al.[8]

TABLE 4: Binding Energies and Vibrational Frequencies of CO Adsorbed on the W(111) Surface[a]

site	state	E_b (eV)	freq (cm^{-1})	red shift (cm^{-1})
1-fold	α	1.37	1920	197
3-fold shallow	α	1.37	1722	395
3-fold deep	α	0.89	1560	557
2-fold bridge	β	1.62	1645	472
inclined C-2:O-1	β	1.79	1318	799
inclined C-5:O-6	β	1.71	1386	731
inclined C-5:O-4	β	1.60	1467	650

[a] The red shifts are measured relative to the computed gas phase CO vibrational frequency of 2117 cm^{-1}.

We have performed calculations for CO adsorption on (1 × 1) and (2 × 2) ad-layers, corresponding to coverages of 1 and $^1/_4$ ML, respectively. The coverage effect is quite small, giving less than 0.1 eV difference in E_b. This is because the (111) surface of a bcc metal is very open. In contrast, the (111) surface of a fcc metal is close-packed and the coverage has a significant effect on the binding energy.[25]

Table 3 shows that the 4th−7th layers play a very important role in the adsorption. For example, on the 1-fold site, the calculated binding energy without taking the 4th−7th layers into account gives an error of 0.99 eV. Therefore, the results of Ryu et al.,[8] computed with only three layers, are not accurate.

We have compared our calculations with two different experimental studies of CO on the W(111) surface.[6,7] These studies present TPD spectra that are not exactly consistent with one another. We have transformed the TPD results to binding energies, by using both a standard Redhead analysis[26] and the Polanyi−Wigner equation.[27,28] Both methods give very similar results. Chen and co-workers[6] found that CO molecularly desorbs at 293 K at a heating rate of 3 K s^{-1}, which corresponds to a binding energy of 0.79 eV. Lee and co-workers[7] observed the desorption of CO at 400 K at the heating rate of 8 K s^{-1}, which corresponds to a binding energy of 1.13 eV. Better estimates of the binding energy can be made if the coverage and heating rates are varied in the experiments. This was not done in either of the experimental papers, and therefore, we use a simple Redhead analysis to give reasonable estimates for the binding energies from the information available.

Chen and co-workers have measured HREEL spectra of CO adsorption on the W(111) surface.[6] Two dominant peaks are observed close to 400 and 2060 cm^{-1} for $T \leq 230$ K. In addition, a broad band ranging from about 1000 to 1600 cm^{-1} is also present. According to previous experimental and theoretical studies of CO adsorption on other transitional metals, e.g., Fe(110) and Fe(111) surfaces,[3,4] the ∼400 cm^{-1} peak is assigned to the W−CO vibrational mode, ∼2060 cm^{-1} to the C−O stretching mode of the α state CO, and the broad band to the C−O stretching mode in the β state CO.

Our calculated binding energies and vibrational frequencies for CO adsorbed on different sites are reported in Table 4. In accordance with convention, we define the α state as end-on adsorption with the C−O bond oriented parallel to the surface normal and the β state as being inclined with respect to the surface normal. The 2-fold bridge state is similar to the C-5:O-6 state, but has a smaller tilt angle. Among the seven binding sites considered, the β state CO in the C-2:O-1 configuration has the highest binding energy (1.79 eV) and also the lowest C−O stretching frequency (1318 cm^{-1}). The binding energies for β states range from 1.6 to 1.79 eV and display stretching frequencies from 1318 to 1645 cm^{-1}. These values are in reasonable agreement with the experimentally observed vibrational band between about 1000 and 1600 cm^{-1}.[6] The experimental and calculated gas-phase C−O frequencies are 2143 and 2117 cm^{-1}, respectively. Hence, the red shifts measured experimentally range from about 500 to 1100 cm^{-1}, while the calculated red shifts range from about 470 to 800 cm^{-1}. The large red shifts are due to the weakening of the C−O triple bond,[5,8] which indicates that the β state CO is the mostly likely precursor to dissociation.

The 1-fold (on-top) and 3-fold shallow are the most favorable α sites; both have binding energies of 1.37 eV (Table 4). In both cases, the adsorbed CO pulls the substrate W atom 0.04−0.06 Å out of the surface. These binding energies are somewhat larger than energies calculated from Redhead analysis of the TPD data of Chen and co-workers (0.79 eV) and of Lee et al. (1.13 eV). The discrepancy between our results and the experimental data may be due to limitations of the Redhead analysis or to overbinding on the part of the DFT calculations. The calculated C−O vibrational frequencies for the two sites are 1930 and 1722 cm^{-1}, respectively, as shown in Table 4. These frequencies are considerably lower than the experimental peak at ∼2060 cm^{-1}, which is red shifted by 83 cm^{-1} from the gas-phase C−O stretch.[6] The larger red shifts seen in the calculations may be the result of DFT overbinding. The 3-fold deep site has a smaller E_b but a much larger C−O frequency red shift.

TABLE 5: Binding Energies and Relative Stabilities for Atomic Carbon and Oxygen Adsorption on the W(111) Surface[a]

	C		O	
site	E_b	δE	E_b	δE
1-fold	5.31	2.04	6.29	0
3-fold shallow	5.30	2.11	5.50	0.79
3-fold deep	6.20	1.21	6.01	0.28
2-fold bridge	7.41	0	5.96	0.33

[a] All energies are in eV.

C. Carbon and Oxygen Adsorption. We have studied the structures and energetics of adsorbed C and O atoms on the W(111) surface as part of our study of CO dissociation. The calculated binding energies are summarized in Table 5, which lists the binding energies of the atoms at $^1/_4$ ML coverage and δE, the energy relative to the most favorable binding site. The 1-fold on-top site is the most favorable binding site for an oxygen atom, while the 2-fold bridge site is the most favorable binding site for a carbon atom. The coadsorption of C and O on their most favorite sites has also been examined and the optimized configuration was used as the final state for CO dissociation calculations. The coadsorption energies are the same as the $^1/_4$ ML coverage binding energies to within a few millielectronvolts. This is consistent with the observation above that the coverage effect for CO adsorption in going from $^1/_4$ to 1 ML is very small. In contrast, Li et al. found that the coadsorption interaction energies for C and O on the Ni(111) surface are larger than 1 eV.[29]

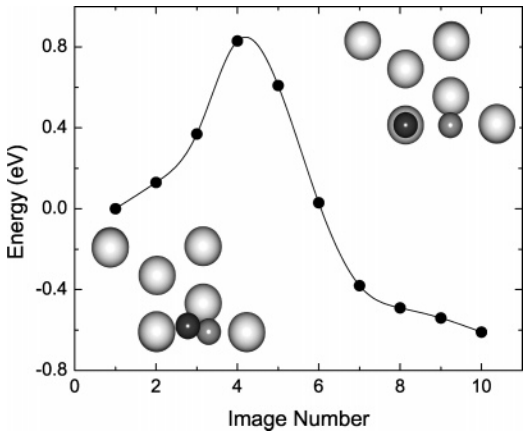

Figure 3. Dissociation of CO on the W(111) surface from the C-2:O-1 β state. The insets show the initial (left) and final (right) states. The line is drawn as a guide to the eye.

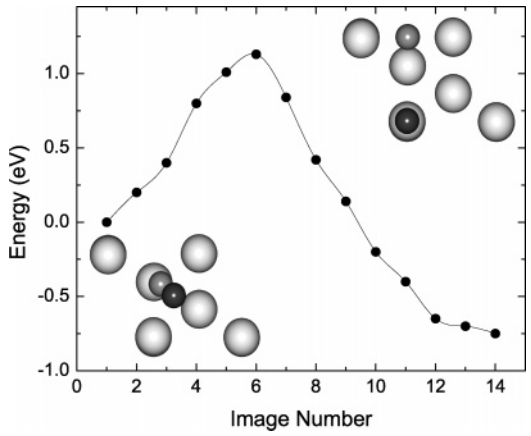

Figure 4. Dissociation of CO on the W(111) surface from the C-5:O-6 β state. The insets show the initial (left) and final (right) states. The line is drawn as a guide to the eye.

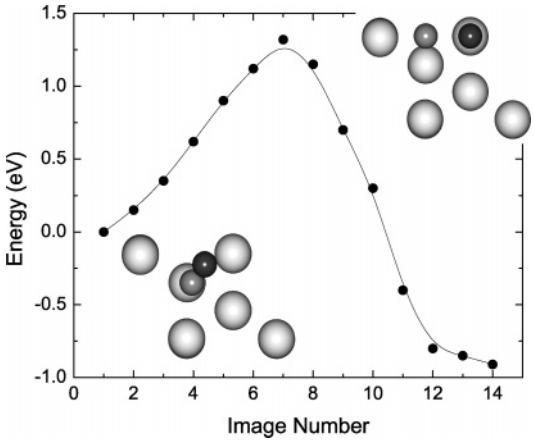

Figure 5. Dissociation of CO on the W(111) surface from the C-5:O-4 β state. The insets show the initial (left) and final (right) states. The line is drawn as a guide to the eye.

The carbon modified W(111) surface was studied by Chen and co-workers because of its potential application in fuel cells.[6] Their TPD study shows that the carbon modified surface is apparently unable to dissociate CO. We have used the carbon preadsorbed W(111) surface as a model for the carbon modified surface in our calculations in order to understand why the carbon modified surface is nonreactive toward CO dissociation. Our findings are discussed in the following section.

D. CO Dissociation. Previous studies have shown that perpendicularly adsorbed CO (α state) desorbs molecularly without dissociation at high temperature.[30] The inclined CO (β) is believed to dissociate due to strong interactions with the d-band of the substrate metals. As mentioned above, our calculations show that the β states have higher binding energies and larger red shifts than the α states, which indicates weakening of the C−O bond. Consequently, we have calculated the minimum energy paths corresponding to dissociation of CO starting from three inclined configurations. Three possible minimum energy paths were constructed by connecting three initial β states to final states with atomic carbon and oxygen adsorbed in their most favorable binding sites. The last three β states listed in Table 4 were chosen as the initial states for dissociation calculations. In each NEB calculation, we used from 8 to 14 linearly interpolated images along the reaction path in addition to the initial and final points. The reaction pathway starting from the inclined configuration C-2:O-1 is shown in Figure 3. The left and right insets show the initial and final states, respectively. Fitting the data along the energy curve yields a dissociation barrier of 0.82 eV. Chen and co-workers[6] found evidence that CO dissociates rapidly around 330 K. Our calculated activation energy agrees very well with this experimental observation. Figures 4 and 5 show the minimum energy dissociation pathways from the inclined configurations C-5:O-6 and C-5:O-4, respectively. The calculated activation energies are 1.19 and 1.41 eV, respectively. The C-2:O-1 configuration is the most likely precursor to dissociation because it has a significantly lower activation energy than the other two β states identified in this work. All the transition states observed in our calculations are "early" in the sense that the structure of the transition state is quite similar to the initial state. For example, the C−O bond length increases from 1.28 to 1.46 Å in going from the initial to the transition state for C-2:O-1 in Figure 3.

An analysis of the structure of CO in the C-2:O-1 configuration shows that the carbon atom is located close to the 2-fold bridge site, but closer to the W atom labeled 2 in Figure 1. According to our atomic carbon and oxygen adsorption calculations, carbon atoms are most likely to occupy the 2-fold bridge sites, having a binding energy that is 1.21 eV larger than the next most favorable site. Therefore, adsorbed carbons may block the adsorption of dissociative β state CO molecules. Moreover, C/W(111) has all favorable final states for C blocked so that dissociation from any β state is inhibited. Only the 1-fold sites are accessible to CO adsorption on the carbon modified surface. This blockage mechanism helps explain the experimental observation that the C/W(111) surface is inactive to CO dissociation.[6]

E. CO/C/O Diffusion. We have investigated the diffusion of CO, atomic oxygen, and atomic carbon on the clean W(111) surface by using the NEB method.[21,22] For each adsorbate, we selected the most favorable binding state as the initial state and the second most favorable binding state as the final state. Diffusion from the 3-fold shallow site to the 1-fold site has a calculated barrier energy of 0.76 eV. This low activation barrier suggests that the migration of CO between various end-on (α state) configurations is facile at moderate temperatures. The diffusion energy barrier from the C-2:O-1 β site to the 1-fold α site is plotted in Figure 6. The diffusion barrier is about 1.42 eV in going from the β to the α state, and about 1 eV for the reverse path. The calculated diffusion barrier for a carbon atom from the 2-fold bridge site to the 3-fold deep site is 1.91 eV. The calculated diffusion barrier for an oxygen atom moving from the 1-fold site to the 3-fold deep site is 0.69 eV. The strong binding energy and relatively high diffusion barrier of carbon indicate that carbon atoms are effectively frozen in the 2-fold

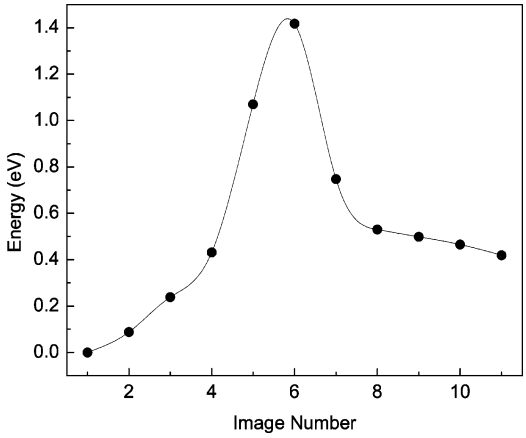

Figure 6. Diffusion pathway of CO on the W(111) surface from the C-2:O-1 β site to the 1-fold α site. The line is drawn as a guide to the eye.

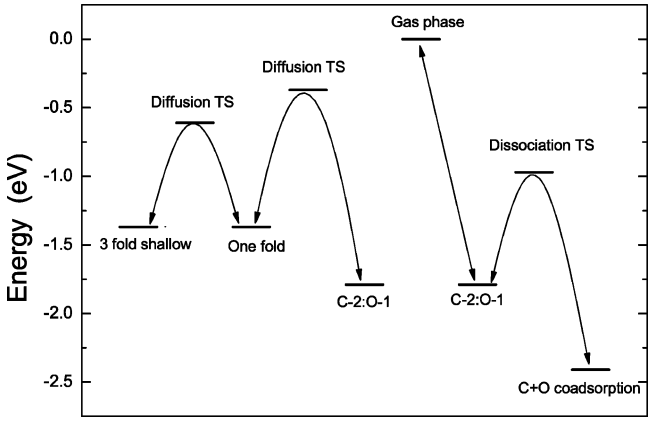

Figure 7. A schematic of the energy landscape for adsorption, diffusion, and dissociation. Only a few selected states are shown.

site at moderate temperatures. The hopping rate for C moving from the 2-fold bridge site to the 3-fold deep site is 8.2×10^{-20} s^{-1} at room temperature, assuming a prefactor of 10^{13} s^{-1}. In contrast, we predict that oxygen atoms are able to diffuse freely on the surface at room temperature. For example, the hopping rate for O moving from the 1-fold to the 3-fold deep site is 1.7 s^{-1} at 300 K. It would be interesting to see experimental verification of our predictions, perhaps by STM measurements.

IV. Conclusions

We have studied the adsorption and diffusion of C, O, and CO on the W(111) surface using density functional theory. A summary of our findings is presented schematically in Figure 7 as an energy landscape diagram for a few selected states. We have computed dissociation pathways for CO on the W(111) surface. Atomic oxygen is preferentially adsorbed on the 1-fold on-top site, but can diffuse to other adsorption sites at room temperature. In contrast, atomic carbon is most strongly adsorbed on the 2-fold bridge site and is essentially immobile on the surface except at elevated temperatures. Molecular CO can be adsorbed in α states, with the C−O bond aligned parallel to the surface normal, or in β states, inclined to the surface normal. The β states have the highest binding energies and the largest C−O stretching frequency red shifts, and are predicted to be the precursor states for dissociation. The lowest calculated dissociation barrier is 0.82 eV, which is consistent with experimental TPD studies. We predict that CO dissociation will result in a self-poisoning process, whereby C blocks further dissociation of CO on the surface. This blockage also explains the experimental observation that the C/W(111) surface is inactive toward CO dissociation.[6]

Finally, our calculations account for the experimental observation that dissociated CO on the W(111) surface does not recombine until ~900 K.[6] We take the dissociation and recombination of the C-2:O-1 β state, shown in Figure 3, as an example. The dissociation energy barrier is $E_{dis} = 0.82$ eV, the recombination energy barrier is $E_{rec} = 1.44$ eV, and the desorption energy, given in Table 4, is $E_{des} = 1.79$ eV. The desorption rate can be approximated as

$$r_{des} = \frac{k_{rec}\, k_{des}}{k_{dis} + k_{des}} [C][O] = k_{eff}[C][O] \qquad (1)$$

where

$$k_{eff} = \frac{k_{rec}\, k_{des}}{k_{dis} + k_{des}} \propto \exp\left(\frac{-E_{eff}}{k_B T}\right) \qquad (2)$$

where k_B is the Boltzmann constant, T is the absolute temperature, and

$$E_{eff} \approx E_{rec} + E_{des} - E_{dis} = 2.41 \text{ eV} \qquad (3)$$

We have assumed that $k_{dis} \gg k_{des}$ and that the prefactor is the same for each of the steps. The effective desorption energy barrier of 2.41 eV is consistent with the observed high temperature required of recombination, assuming a typical prefactor of 10^{13} s^{-1}.

Acknowledgment. We thank Jan Steckel for helpful comments and discussions. We acknowledge the National Energy Technology Laboratory for support of this work.

References and Notes

(1) Somorjai, G. A. *Introduction to Surface Chemistry and Catalysis;* Wiley: New York, 1994.
(2) Claridge, J. B.; York, A. P. E.; Brungs, A. J.; Marques-Alvarez, C.; Sloan, J.; Tsang, S. C.; Green, M. L. H. *J. Catal.* **1998**, *180*, 85.
(3) Mehandru, S. P.; Anderson, B. *Surf. Sci.* **1988**, *201*, 345.
(4) Bartosch, C. E.; Whitman, L. J.; Ho, W. *J. Chem. Phys.* **1986**, *85*, 1052.
(5) Sorescu, D. C.; Thompson, D. L.; Hurley, M. M.; Chabalowski, C. F. *Phys. Rev. B* **2002**, *66*, 035416.
(6) Hwu, H. H.; Polizzotti, B. D.; Chen, J. G. *J. Phys. Chem. B* **2001**, *105*, 10045.
(7) Lee, S.; Kim, Y.; Yang, T.; Boo, J.; Park, S.; Lee, S.; Park, C. *J. Vac. Sci. Technol. A* **2000**, *18*, 1455.
(8) Ryu, G. H.; Park, S. C.; Lee, S.-B. *Surf. Sci.* **1999**, *427−428*, 419.
(9) Anderson, A. B. *J. Chem. Phys.* **1975**, *62*, 1187.
(10) Anderson, A. B.; Grimes, R. W.; Hong, S. Y. *J. Phys. Chem.* **1987**, *91*, 4245.
(11) Kresse, G.; Hafner, J. *Phys. Rev. B* **1994**, *49*, 14251.
(12) Kresse, G.; Furthmuller, J. *Comput. Mater. Sci.* **1996**, *6*, 15.
(13) Kresse, G.; Furthmuller, J. *Phys. Rev. B* **1996**, *54*, 11169.
(14) Perdew, J. P.; Burke, K.; Ernzerhof, M. *Phys. Rev. Lett.* **1996**, *77*, 3865.
(15) Zhang, Y.; Yang, W. *Phys. Rev. Lett.* **1998**, *80*, 890.
(16) Perdew, J. P.; Chevary, J. A.; Vosco, S. H.; Jackson, K. A.; Pederson, M. R.; Singh, D. J.; Fiolhais, C. *Phys. Rev. B* **1992**, *46*, 6671.
(17) Hammer, B.; Hansen, L. B.; Nørskov, J. K. *Phys. Rev. B* **1999**, *59*, 7413.
(18) Kresse, G.; Joubert, J. *Phys. Rev. B* **1999**, *59*, 1758.
(19) Blochl, P. E. *Phys. Rev. B* **1994**, *50*, 17953.
(20) Monkhorst, H. J.; Pack, J. D. *Phys. Rev. B* **1976**, *13*, 5188.
(21) Mills, G.; Jónsson, H.; Schenter, G. K. *Surf. Sci.* **1995**, *324*, 305.
(22) Jónsson, H.; Mills, G.; Jacobsen, K. W. Nudged Elastic Band Method for Finding Minimum Energy Paths of Transitions. In *Classical and Quantum Dynamics in Condensed Phase Simulations*; Berne, B. J., Ciccotti, G., Coker, D. F., Eds.; World Scientific: River Edge, NJ, 1998.
(23) Xu, W.; Adams, J. B. *Surf. Sci.* **1994**, *319*, 45.

(24) Holzwarth, N. A. W.; Chervenak, J. A.; Kimmer, C. J.; Zheng, Y.; Xu, W.; Adams, J. B. *Phys. Rev. B* **1993**, *48*, 12136.
(25) Shah, V.; Li, T.; Baumert, K. L.; Cheng, H.; Sholl, D. S. *Surf. Sci.* **2003**, *217*, 537.
(26) Bartosch, C. E.; Whitman, L. J.; Ho, W. *J. Chem. Phys.* **1986**, *85*, 1052.
(27) Lee, J. G.; Ahner, J.; Yates, J. T. *J. Chem. Phys* **2001**, *114*, 1414.
(28) Polanyi, M.; Wigner, E. *Z. Phys. Chem.* **1928**, *139*, 439.
(29) Li, T.; Bhatia, B.; Sholl, D. S. *J. Chem. Phys.* **2004**, *121*, 10241.
(30) Mortensen, J. J.; Hansen, L. B.; Hammer, B.; Nørskov, J. K. *J. Catal.* **1998**, *182*, 479.